Proceedings of the XVII ECSMGE-2019
Geotechnical Engineering foundation of the future
ISBN 978-9935-9436-1-3

doi: 10.32075/17ECSMGE-2019-0223

XVII European Conference
ECSMGE 2019
Reykjavik
on Soil Mechanics
and Geotechnical Engineering

Granular strength and gradation effects on self-supported unconfined sand specimen

Effets de la résistance et de la gradation granulaires sur un échantillon de sable auto-supporté non confiné

Oliver-Denzil S. Taylor, PhD, P.E.
U.S. Army Corps of Engineers, Vicksburg, United States

Woodman W. Berry, P.E.
U.S. Army Corps of Engineers, Vicksburg, United States

ABSTRACT: Laboratory research on non-plastic soil behaviour for low to zero confinement environments relies on the use of effective stress principles and geotechnical laboratory testing equipment to infer behaviour. Research suggests that the use of effective stress principles are not indicative of near-surface environments due to the application of confining pressures, to maintain sample stability of granular material greater than 0.5-mm dia., where suction and tensile strengths are believed to be negligible. In-situ cases, e.g., open trench excavations, show that these sands can maintain an unconfined self-supported vertical face. To evaluate granular strength characteristics at ultralow confinement without the influence of fines, suction, or cementation, thirty-six unconfined-drained tests were conducted on dry, loose to medium-dense sand at various gradations between 0.638- and 5.55-mm nominal dia. The results indicate that interlocking particle chains can resist up to a 10-kPa axial load without deformation that cannot be attributed to cementation, suction, or dilatancy. Further, these results suggest that for dry granular material, the actual Mohr failure envelope does not pass through the origin, as is assumed in soil mechanics thoery.

RÉSUMÉ: Les recherches en laboratoire sur le comportement des sols non plastiques dans des environnements à confinement faible à zéro reposent sur l'utilisation de principes de contrainte efficaces et d'un équipement de test de laboratoire géotechnique pour en déduire le comportement. Les recherches suggèrent que l'utilisation de principes de contrainte efficaces n'est pas indicative des environnements proches de la surface en raison de l'application de pressions de confinement, afin de maintenir la stabilité de l'échantillon de matériau granulaire supérieure à 0,5 mm de dia., les résistances à la traction et à la traction étant considérées comme négligeables. Les cas in situ, par exemple les excavations en tranchée à ciel ouvert, montrent que ces sables peuvent maintenir une face verticale auto-supportée non confinée. Pour évaluer les caractéristiques de résistance granulaire au confinement ultra-faible sans l'influence des particules fines, de l'aspiration ou de la cimentation, trente-six essais avec drainage non confiné ont été effectués sur du sable sec, lâche à moyennement dense, à différentes gradations comprises entre 0,638 et 5,55 mm (dia. nominal). Les résultats indiquent que des chaînes de particules imbriquées peuvent résister à une charge axiale allant jusqu'à 10 kPa sans déformation qui ne peut être attribuée à une cémentation, à une aspiration ou à une dilatance. De plus, ces résultats suggèrent que pour les matériaux granulaires secs, l'enveloppe de rupture réelle de Mohr ne passe pas par l'origine, comme il est supposé dans la théorie de la mécanique des sols.

Keywords: granular shear strength, laboratory testing, unconfined soils

1 INTRODUCTION

Research into the shear strength, τ, in low confiment evironments suggests that the impact of suction to the overall shear strength can be treated as an additive component to conventional saturated effective strss relationships, e.g., Equation 1 [Vanapalli et al. 1996; Han and Vanapalli 2016].

$$\tau = c' + (\sigma_n - u_a)\tan(\phi') + \psi S_r^{\xi}\Gamma \qquad (1)$$

In the above equation, σ_n is the normal stress along the failure plane, u_a is the pore air pressure, c' is the soil cohesion, ϕ' is the effective internal friction angle, and $\psi S_r^{\xi}\Gamma$ is the contribution of non-linear suction strength from the SWCC in unsaturated soil mechanics [Vanapalli et al. 1996; Han and Vanapalli 2016]. Han and Vanapalli [2016] suggest that for shear strength calculations, the Γ term is assumed equal to $\tan(\phi')$, the ξ parameter is 1.0, and S_r is the saturation for sand. Lu et al. [2010a] presented a similar equation based on an effective saturation, S_e, the Mohr-Coulomb failure criterion, and the van Genuchten [1980] SWCC fitting parameters, n and α.

$$\tau = \left[(\sigma - u_a) + \frac{S_e}{\alpha}\left(S_e^{\frac{n}{1-n}} - 1\right)^{\frac{1}{n}}\right]\tan\phi' + c' \qquad (2)$$

For most geotechnical problems, these equations yield relatively accurate approximations of shear strength behaviour [Lu et al. 2010b; Han and Vanapalli 2016]. However, Taylor et al. [2018] showed that the shear strength suggested by equations 1 and 2 does not reflect the observed shear strengths within for unconfined medium to fine sands. Furthermore, the effective shear expressions are not representative of the underlying physics or actual behaviour of unconfined or near-surface soils, exposing the limitations of effective stress expressions as noted by Santamarina [2001]. Changes to the inter-particle stresses in the near surface, or uppermost meter of the earth, have a first-order effect on the quantification of a soil's structure or fabric used to calculate strength characteristics and elastic moduli that govern modeled behavior [Taylor et al. 2014; Taylor et al. 2018].

Taylor et al. [2018] did not investigate the shear strength of coarse granular material where suction effects, equations 1 and 2, are considered negligable [Lu et al. 2010b]. For dry granular materials, the actual Mohr failure envelope is assumed to pass through the origin, i.e., the soil will not stand as a cylinder if the confining pressure is zero and is central to the mechanical theory of equations 1 and 2. Therefore, this paper present the laboratory findings of unsupported dry sand specimens at different ratios of a medium sand (0.638-mm nominal particle diamter) to coarse sand (3.38-mm nominal diameter) and fine gravel (5.55-mm nominal diameter) silica-quartz particles to examine the validity of the assumption that unconfined coarse granular material does not possess shear resistance.

2 LABORATORY TESTING

2.1 Specimen Material

The material used in this study is a silica-quartz sand that undewent a series of wet/dry seives to separate the grain sizes into the desired nominal diameters and ensure no fines or non-nominal particles are present within each grain-size category, Figure 1.

A blend, percent by weight of 0.638-mm (nominal) particles to both coarse sand and fine

Figure 1. Grain size and shapes used in this study for distribution gradations. The scale shown is in centi-metres.

gravel, nominally 3.38- and 5.55-mm diameter grains, respectively, was constructed to examine the effects of particle gradation and maximum grain size on the fabric strength, i.e., the interlocking structural particle chains.

2.2 Specimen Preparation

The remolded samples were prepared using an energy-based undercompaction method as outlined in Taylor et al. [2017; 2018]. This method was employed to prepare the samples in a highly repeatable manner with uniform densities, moisture contents and soil fabric throughout the specimen. Two different compactive energies, 200 kJ/m^3 and 600 kJ/m^3, were used to create loose and medium dense specimens, respectively.

All specimens were constructed to a height of 145 mm and 71 mm in diameter using a split mold lined with parchment paper. The specimens are built in four lifts at a reconstitution saturation of 24%.

To eliminate the influence of matric suction, samples must be void of moisture such that only granular friction provides resistance to applied and gravitational stresses. Taylor et al. [2018] illustrated that similar samples air-dried for a minimum of 48 hours yielded equivalent gravimetric water contents compare with oven-dried specimens to a gravimetric water content accuracy of ±0.01% in accordance with ASTM Standard Test Method D2216. Figure 2 shows

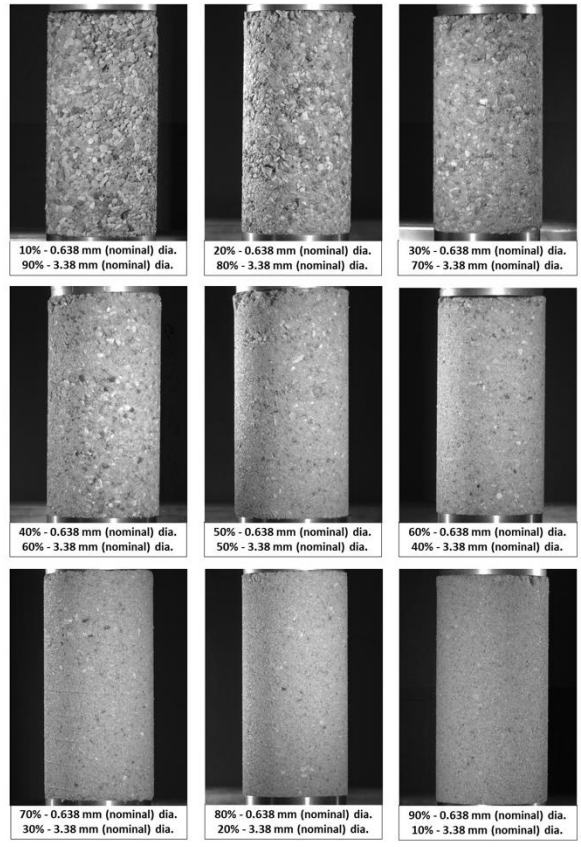

Figure 2. Reconstituted specimen for each 0.638/3.38 mm blend remolded at a compactive energy of 600 kJ/m^3.

the final reconstituted specimens at each particle gradation tested for the 0.638/3.38-mm blended material. To ensure that the specimens were dry, moisture content samples were taken immediately post failure.

2.3 Testing Procedure

After air-dring in a controlled environment for 48 hours, the specimens were carefully loaded using precision weights, with a 20-second time lag between load applications, until failure as prescribed by Taylor et al. [2018]. The amount of weight held before failure and the amount of weight at failure were recorded. The maximum axial load supported without failure is presented herein.

Each test was recorded by high-speed high-resolution videography (two cameras at a 1280x800 dpi resolution and 389 fps). Still-frame images at 1280x800 dpi resolution were created and enhanced to 150% of the sample dimensions for determining specimen strains via pixel matching, i.e., computer-aided and manually.

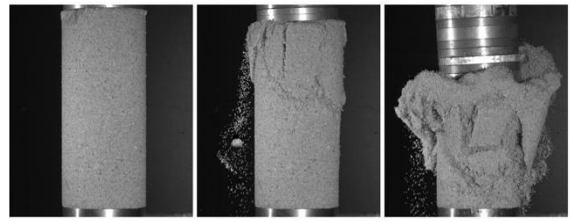

Figure 3. Still-frame images from the high-speed videography for failure of a 0.368/5.55 mm blend at a mixture ratio of 90/10 respectively and compactive energy of 600 kJm^3.

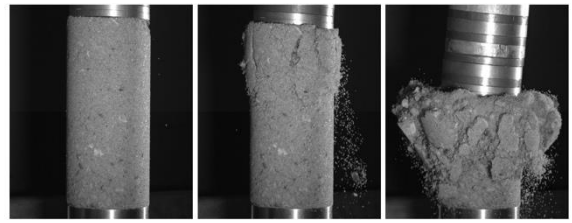

Figure 4. Still-frame images from the high-speed videography for failure of a 0.368/5.55 mm blend at a mixture ratio of 60/40 respectively and compactive energy of 200 kJm^3.

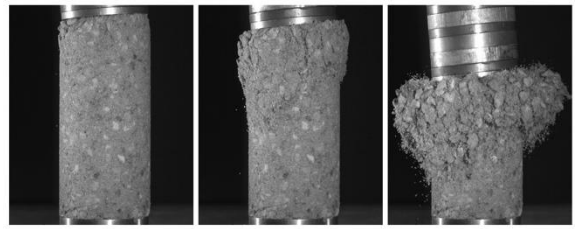

Figure 5. Still-frame images from the high-speed videography for failure of a 0.368/5.55 mm blend at a mixture ratio of 40/60 respectively and compactive energy of 200 kJm^3.

Figure 6. Still-frame images from the high-speed videography for failure of a 0.368/5.55 mm blend at a mixture ratio of 20/80 respectively and compactive energy of 600 kJm^3.

3 TESTING RESULTS

3.1 Failure Mode Observations

As observed by Taylor et al. [2018], the dry material exhibited a brittle radially expansive progressive failure wherein only the upper portion of the specimen exhibited deformations, repesentative imagery is shown in Figures 3-6 for the 0.368/5.55-mm blendend material. The weights fell along the center vertical axis indicating the lack of shear plane development. Under the high-speed videography, it is readily observed that the particle independently rotate in a clock-wise direction and are ejected in an initially horizontal trajectory. This implies that there is a lack of cementation within the specimens and that the resulting material strength is the function of interlocking particle chains, i.e., the soil fabric. No strains were observed prior to the initialization of failure.

3.2 Soil Fabric Strength

The axial load held prior to the initialization of failure is given in Table 1. The general trend is that the specimens with gradations of 90% 0.638 mm and 10% coarse material yielded the highest strength. However, it was also observed that specimens at 60% 0.638-mm and 40% coarse material typically yielded a similar soil fabric strength. Only one specimen at 10% 0.638 was able to remain standing under gravity stresses.

Overall, the data suggests an independency on the material density and a dependency on the particle gradation to median fabric strength, Figure 7. Table 1 suggests that the larger the coarse grain size the greater the maximum

Table 1. Axial load held without detectable starining of reconstituted specimen for each gradation tested in this study.

Pecentage of Specimen Comprised of 0.638 mm Particles	Nominal Coarse Particle Dia. 3.38 mm Axial Load Held, kPa Loose	3.38 mm Axial Load Held, kPa Medium Dense	5.55 mm Axial Load Held, kPa Loose	5.55 mm Axial Load Held, kPa Medium Dense
90%	5.3	1.1	9.2	9.8
80%	6.5	6.8	5.5	8.7
70%	4.1	3.3	8.2	6.0
60%	4.2	7.8	9.0	7.0
50%	5.6	3.6	4.3	6.2
40%	5.5	4.2	7.6	3.7
30%	3.5	1.9	3.1	0.9
20%	5.7	3.5	0.4	1.4
10%	0.0	1.8	0.0	0.0

magniude of the soil fabric strength. However, for the two coarse material sizes, there isn't a significant difference in the range of potential soil fabric strength for this dataset. Therefore, the soil fabric strength is presented as a function of the precentage of the soil matrix comprised of 0.638-mm (nominal) particles over which a signiicant diffence in supported axial load is observed, Figure 7. This function is representative of the grain-to-grain contact area within the specimen. Generally, the larger the 0.638-mm fraction, the stronger the specimen; this is not always true. The data suggests that the greater the 0.638-mm fraction, i.e., lower the void rato, the greater the potential for the development of tightly interlocking particle chains. Figure 7 illustrates the potential relationship between the medium sand fraction and the median fabric strength, independent of the size of the coarse fraction. Of interest is that the mean soil farbic strength does not increase post the 60% 0.638-mm and 40% coarse material blend.

4 IMPLICATIONS

The soil fabric strength within the upper meter of the subsurface is critical to a broad range of military and civilian missions spaces. Current effective stress equations, e.g., equations 1 and 2, do not adequately represent the in situ behavior, e.g., the theoretical failure surface in a shallow trench collapse is rarely consistent with field observations [Taylor et al. 2018; Taylor and LaBaw 2018]. Similar observations have been made for wave propagation and munition penetration as well as clandestine tunnel stability [Sloan et al. 2010; Taylor et al. 2014; Song et al. 2017].

These findings illustrate that under zero confinement, there can exist a significant shear

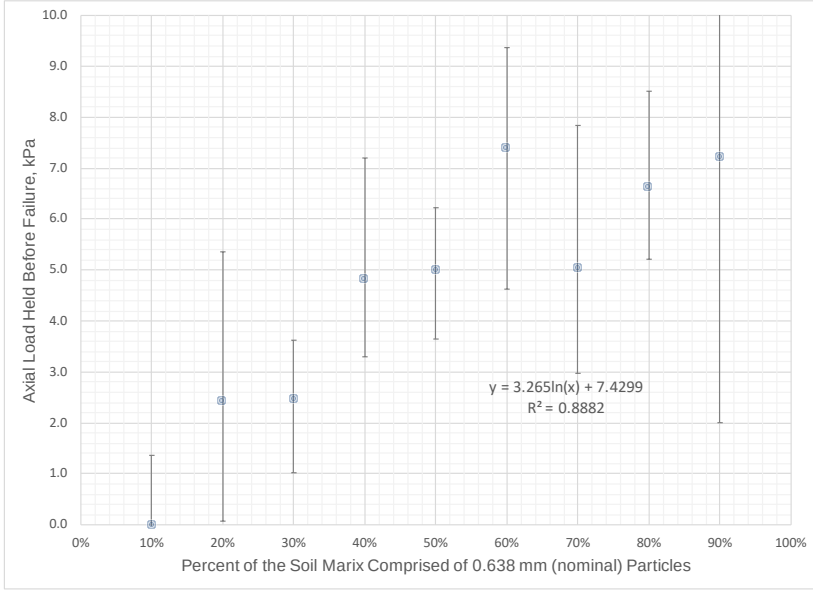

Figure 7. Relationship between the percent of the soil matrix comprised of 0.638-mm diameter material and the axial load held before failure was initiated.

resistance of up to approximately 10 kPa, Figure 7. Furthermore, these findings suggest that deformations may not be directable prior to a catastrophic failure while carrying an unconfined load. Moreover, these results illustate an explaination of close proximity near-surface soil strength variability wherein no discernable difference in in-situ characteristics are measured.

5 CONCLUSIONS

Thirty-six unconfined-drained tests were conducted on dry, loose to medium-dense sand, at various gradations between 0.638 and 5.55 mm (nominal dia.). The results indicate that interlocking particle chains can resist up to a 10-kPa axial load without deformation that cannot be attributed to cementation, suction, or dilatancy. Further, these results suggest that, for dry granular material, the actual Mohr failure envelope does not pass through the origin, as is assumed in soil mechanics thoery.

6 ACKNOWLEDGEMENTS

The authors would like to aknowledge M.D. Antwine and W.R. Rowland for their assistance in conducting the experiments. Funding was provided by the ERDC Future Inovations Fund: *Unlocking the physics of near-surface soil mechanics*. Permission to publish was granted by Director, Geotechnical and Structures Laboratory, U.S. Army Engineer Research and Development Center, with unlimited distribution.

7 REFERENCES

ASTM D2216-10 (2010). Standard Test Methods for Laboratory Determination of Water (Moisture) Content of Soil and Rock by Mass, Annual Book of ASTM Standards, ASTM Inernational, West Conshohocken, PA.

Han, Z., and Vanapalli, S.K. (2016). Stiffness and shear strength of unsaturated soils in relation to soil-water characteristic curve. *Geotechnique* 66(8), 627-647.

Lu, N., Godt, J.W., and Wu, D.T. (2010a). A closed-form equation for effective stress in unsaturated soil. *Water Resources Research*, 46, W05515.

Lu, N., Wu, B., and Tan, C.P. (2010b). Tensile strength characteristics of unsaturated sands. *J. of Geotech. and Geoenviron. Eng.* 133(2): 144-154.

Santamarina, J.C. (2001). Soil Behavior at the Microscale: Particle Forces. *Proc. Symp. Soil Behavior and Soft Ground Construction*, in honor of Charles C. Ladd - October 2001, MIT, 1-32.

Sloan, S.D., Peterie, S.L., Miller, R.D., Ivanov, J., Schwenk, J.T.,, and McKenna, J.R. (2015). Detecting clandestine tunnels using near-surface seismic techniques. *Geophysics*, 80(5), 127-135.

Song, A.J., West, B.A., Taylor, O.-D.S., O'Connor, D.T., Parno, M.D., Hodgdon, T.S., Cole, D.M., and Clausen, J.L. 2017. Munition Penetration-Depth Prediction: SERDP SEEDC Project MR-2629, ERDC/CRREL Technical Report TR-17-12.

Taylor, O-D.S., McKenna, M.H., Kelley, J., Berry, T., Quinn, B., and McKenna, J. (2014). Partially saturated soil causing variability in near surface seismic signals: a case history. *Near Surface Geophysics*, 12(4), 467-480.

Taylor, O.-D.S., Berry, W.W., Winters, K.E., Rowland, W.R., Antwine, M.D., and Cunningham, A.L. 2017. Protocol for cohesionless sample preparation for physical experimentation. *Geotechnical Testing Journal* 40(2): 284-301.

Taylor, O.-D.S., Winters, K.E., Berry, W.W., Walshire, L.A., and Kinnebrew, P.G. (2018) Near-surface soils: Self-supported unconfined drained sand specimen. *Can. Geotech. J.* https://doi.org/10.1139/cgj-2017-0261.

Taylor, O.-D.S., and LaBaw, S.M. (2018). Emergency trench shoring and rescue: A simplified method for calculating lateral earth pressures. *Advances in Civil Engineering*, Vol. 2018, ID: 5280926

van Genuchten, M. T. (1980), A closed-form equation for predicting the hydraulic conductivity of unsaturated soils. *Soil Sci. Soc. Am. J.*, 44, 892–898.

Vanapalli, S.K., Fredlund, D.G., Pufahl, D.E., and Clifton, A.W. (1996). Model for the prediction of shear strength with respect to soil suction. *Can. Geotech. J.*, 33(3), 379-392.